Contents lists available at ScienceDirect

Agricultural Water Management

journal homepage: www.elsevier.com/locate/agwat

Modified EC_a – EC_e protocols for mapping soil salinity under micro-irrigation

D.L. Corwin [a,*,1], E. Scudiero [a,b], D. Zaccaria [c]

[a] USDA-ARS, US Salinity Laboratory, 450 West Big Springs Road, Riverside, CA 92507-4617, USA
[b] Department of Environmental Sciences, University of California, Riverside, CA 92521, USA
[c] Department of Land, Air and Water Resources, University of California, Davis, CA 95616, USA

ARTICLE INFO

Handling Editor - Dr. R. Thompson

Keywords:
Apparent soil electrical conductivity
Electromagnetic induction
Electrical resistivity
Proximal sensor
Soil spatial variability
Drip irrigation

ABSTRACT

Climate change will increase the frequency and intensity of drought in water-scarce agricultural areas that rely on irrigation. The increased strain on finite water resources for irrigated agriculture will cause a shift from sprinkler and flood irrigation to micro-irrigation. Micro-irrigation results in complex 3-dimensional salinity patterns. Current field-scale apparent soil electrical conductivity (EC_a) directed soil sampling protocols and guidelines are inadequate for mapping the complex local-scale 3-dimensional nature of salinity resulting from water applications by micro-irrigation systems (i.e., drip, buried drip, micro sprinklers, bubblers, etc.). A field study was conducted to develop additional EC_a-directed soil sampling guidelines to map local- and field-scale variability in salinity under drip-irrigation systems within a commercial nut production orchard (i.e., pistachio orchard) using hard (i.e., salinity or EC_e, electrical conductivity of the saturation extract) and soft data (i.e., geospatial EC_a measurements), which required an accurate EC_a – EC_e calibration. The revised EC_a-directed soil sampling guidelines for drip irrigation on a mature pistachio orchard indicate that a single soil core should be taken 0.9–1.2 m perpendicular to the drip line within the tree root system, rather than at the drip line, to improve the EC_a – EC_e calibration. Calibration of EC_a to EC_e, improved from $R^2 = 0.25$ to $R^2 = 0.73$ for site Flores D01, and from $R^2 = 0.17$ to $R^2 = 0.72$ for site Flores D05. The improved guidelines broaden the scope of application of EC_a-directed soil sampling to map field-scale salinity on orchards under drip irrigation. The information presented is of value and benefit to producers, agriculture consultants, irrigation practitioners, cooperative extension specialists, Natural Resources Conservation Service field staff, and soil and water researchers.

1. Introduction

There is an expectation that climate change will bring increased frequency of extreme weather events around the globe, with unusually high rainfall events leading to floods and low precipitation, higher temperatures, and higher potential ET resulting in longer, harder, and more frequent droughts and larger-magnitude water scarcity. Evidence of the impact of climate change on drought is found worldwide. For instance, the USA has experienced an increase in moderate to severe levels of drought particularly in the Southwest with a megadrought in southwestern North America extending from 2000 to 2021 and comprising the driest 22-year period in 12 centuries (Williams et al., 2022). The most notable recent drought in the USA from a public-awareness perspective due to its impact on agricultural productivity was the California drought of 2011–2016. This caused drastic reductions in irrigation water allocations to farmers in the agriculturally productive San Joaquin Valley and heightened water conservation measures in urban areas, which resulted in continuing the progressive shift from flood and sprinkler irrigated low-cash crops to micro-irrigated high-cash crops including nuts and fruits (e.g., Tindula et al., 2013; Taylor and Zilberman, 2017). This shift was encouraged and supported by provision of federal and state financial incentives to growers such as

Abbreviations: EC_a, apparent soil electrical conductivity (dS m^{-1}); EC_e, electrical conductivity of the saturation extract (dS m^{-1}); EM_h, EC_a measured with electromagnetic induction in the horizontal coil configuration (dS m^{-1}); EM_v, EC_a measured with electromagnetic induction in the vertical coil configuration (dS m^{-1}); EMI, electromagnetic induction; SP, saturation percentage.

* Corresponding author.
E-mail addresses: Dennis.Corwin@usda.gov (D.L. Corwin), Elia.Scudiero@ars.usda.gov (E. Scudiero), dzaccaria@ucdavis.edu (D. Zaccaria).
[1] Senior author.

https://doi.org/10.1016/j.agwat.2022.107640
Received 28 September 2021; Received in revised form 26 March 2022; Accepted 3 April 2022
Available online 27 April 2022
0378-3774/Published by Elsevier B.V.

the Environmental Quality Incentives Program (EQIP) and State Water Efficiency & Enhancement Program (SWEEP). Other recent worldwide droughts include a one-in-a-thousand-year drought in Australia (e.g., lower portion of the Murray-Darling River Basin), which began in 1995 continuing until 2009; Spain's drought in Catalonia; northern India's drought in the first decade of the new millennium; and droughts in northern China, Syria, and southeastern Brazil. Even though there is no short-term extreme weather event that can be conclusively attributed to climate change, there is a statistical record of these events showing that they clearly occur with increased frequency and/or intensity (Dai, 2011). It can be expected that as droughts increase in intensity and frequency in highly productive arid and semi-arid agricultural areas there will be a shift to micro-irrigation systems as a means of coping with water scarcity (e.g., Food and Agriculture Organization FAO, 2012, 2017), as has been the case in California's San Joaquin Valley.

In addition, climate change is globally impacting soil salinity accumulation with some of the greatest potential detrimental impact occurring in water-scarce agricultural areas, such as California's San Joaquin Valley (Corwin, 2021). The accumulation of soil salinity can result in reduced plant growth, reduced yields, and in severe cases, crop failure by reducing the osmotic potential making it more difficult for the plant to extract water. Salinity may also cause specific-ion toxicity (e.g., Na^+ ion toxicity) or upset the nutritional balance of plants. Furthermore, the salt composition of soil water influences the composition of cations on the exchange complex of soil particles, which influences soil permeability and tilth. An inflation-adjusted cost of salt-induced land degradation was estimated at \$441 USD ha^{-1}, resulting in an estimated global economic loss of \$27.3 billion USD for 2013 (Qadir et al., 2014). Welle and Mauter (2017) estimated an income loss due to salinity within California alone at \$3.7 billion USD for 2014. The ability to spatially assess soil salinity will become an even greater concern in the future than it already is today.

Micro-irrigation systems, such as drip irrigation, produce complex local-scale (i.e., $< 3\ m^2$) and field-scale ($< 3\ km^2$) soil salinity patterns. Research by Burt and Isbell (2005), Hanson and May (2011), and Jadoon et al., (2015, 2017) shows the complex patterns of local-scale soil salinity leaching under drip irrigation. Soil salinity patterns emanate from each dripper and follow the water flow and water content patterns illustrated in Fig. 1. At each drip emitter a gradation of soil salinity radiates outward (Fig. 1b) and downward through the soil profile (Fig. 1d) resulting in a complex 3-dimensional distribution of salinity across a field under drip irrigation. Mapping these complex salinity patterns at field scale is a formidable challenge.

Currently, the most common method of mapping salinity at field (i.e., $< 3\ km^2$) and landscape (i.e., 3–10 km^2) scales is geospatial measurements of apparent soil electrical conductivity (EC_a). Apparent soil electrical conductivity is a measure of the electrical conductivity of the bulk soil. It measures anything conductive in the soil. Geospatial EC_a measurements are particularly well suited for establishing within-field spatial variability of not only soil salinity, but a range of soil properties (e.g., water content, texture, organic matter, and bulk density) because they are quick and dependable measurements that integrate the influence of several soil properties contributing to the electrical conductance of the bulk soil (Corwin and Leach, 2005a). At present, no other measurement provides a greater level of spatial soil information than that of geospatial measurements of EC_a when used to direct soil sampling (Corwin and Leach, 2005a). The characterization of spatial variability using geospatial EC_a measurements is based on the hypothesis that spatial EC_a information can be used to develop a directed soil sampling plan that identifies sites that adequately reflect the range and variability of soil salinity and/or other soil properties correlated with EC_a at the study site (Corwin and Lesch, 2003, 2005b). Maps of EC_a variability provide the spatial information to direct the selection of soil sample sites to characterize the spatial variability of those soil properties correlated, either for direct or indirect reasons, to EC_a. In essence, EC_a serves as a surrogate to map those properties that correlate with EC_a at that particular field site. This is referred to as *EC_a-directed soil sampling*. This hypothesis has repeatedly held true for a variety of agricultural applications (Lesch et al., 1992, 2005; Johnson et al., 2001; Corwin and Lesch, 2003, 2005b, 2005c; Corwin et al., 2003a, 2003b; Corwin, 2005).

Current field-scale EC_a-directed soil sampling protocols and guidelines, which were developed by Corwin and Lesch (2005b, 2013) and have been reviewed and summarized by Corwin and Scudiero (2020), were devised for natural precipitation and flood and sprinkler irrigation systems where local-scale variation in soil salinity is less complex since water infiltrating across the soil surface is relatively uniform in comparison to micro-irrigation systems. These EC_a-directed soil sampling protocols and guidelines may be inadequate for mapping the complex local-scale 3-dimensional nature of salinity resulting from micro-irrigation systems (i.e., drip, buried drip, micro sprinklers, etc.).

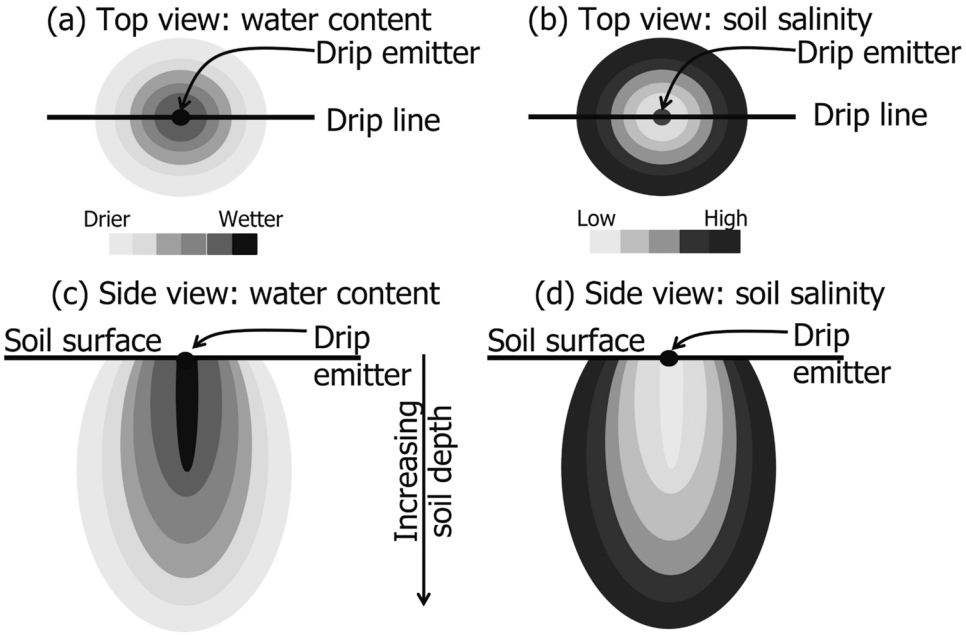

Fig. 1. Top (a, b) and profile (c, d) views of idealized soil water content (a, c) and soil salinity (b, d) distributions under a drip irrigation emitter.

When following the current EC_a-directed soil sampling protocols of Corwin and Lesch (2013) to map field-scale soil salinity for a field under drip irrigation, a single soil core is taken at the location of a drip emitter for selected locations within the field determined from model- (e.g., response surface sample design) or design-based (e.g., stratified random sampling) sample designs based on the spatial variability of EC_a measurements. The soil sample is in the "sweet" spot (i.e., location where the salinity is leached the most and is the lowest), which is not representative of the 1–2 m^3 volume of measurement of the electromagnetic conductivity meter (i.e., Geonics EM38) used to measure EC_a (Fig. 2). As shown in Fig. 2 the induced electromagnetic field encompasses the full salinity gradient created by the drip emitter, resulting in EC_a measurements (i.e., measurement of EC_a in the horizontal coil configuration, EM_h, and in the vertical coil configuration, EM_v) that are not representative of the salinity in the soil core taken directly below the drip emitter. Subsequently, the electrical conductivity of the saturation extract (EC_e) obtained from the soil core sample, which is the customary quantitative measure of soil salinity, is not representative, resulting in an erroneous EC_a to EC_e calibration. To map soil salinity accurately for fields under drip irrigation a modified set of protocols is likely needed that considers the complex local-scale variability in salinity.

Accurate EC_a - EC_e calibrations are essential since hard data from soil cores is not sufficient to map salinity on drip irrigated fields with sufficient spatial accuracy to be meaningful due to the high level of local-scale variability in salinity. The interpolation of salinity from only soil core samples is insufficient even if 100 or more soil cores are taken. Rather, soft data, consisting of thousands of geospatial EC_a measurements that are converted to EC_e through a calibration, are needed to characterize the complex local- and field-scale salinity patterns. Maps with this level of complexity will reveal the local- and field scale salinity patterns that are needed for site-specific irrigation management to control soil salinity. Site-specific irrigation management of drip-irrigation systems provides the level of water management that will be essential in water-scarce agricultural areas that are expected to suffer longer and harsher periods of drought due to climate change.

It is hypothesized that the abrupt local-scale changes in soil salinity that occur under drip irrigation will detrimentally impact the ability to calibrate EC_a to EC_e for a field-scale EC_a survey. The objective of this paper is to evaluate the impact of local-scale changes in soil salinity under drip irrigation upon the calibration of EC_a to EC_e when using the current EC_a-directed soil sampling protocols summarized by Corwin and Scudiero (2020) to map field-scale soil salinity. If current protocols are inadequate, then modifications to the current EC_a-directed soil sampling protocols are proposed based on an analysis of the local-scale variation in soil salinity. The modified EC_a-directed soil sampling protocols will provide improved EC_a to EC_e calibrations for micro-irrigation systems that will better map local-scale soil salinity at and near drip lines, providing detailed micro-irrigation management information for salinity control within the root zone.

2. Materials and methods

A two-phased approach was used at the Flores Farm pistachio orchard near Lemoore, CA: (1) to determine the influence of local-scale changes in soil salinity under drip irrigation upon the EC_a – EC_e calibration and (2) to establish the modifications in the EC_a-directed soil sampling protocols needed to improve the calibration. The approach for evaluating the impact of local-scale variation in soil salinity under a drip irrigation system upon the EC_a - EC_e calibration involved taking a variety of soil cores to establish the "best" soil core or combination of cores that results in the most robust EC_a - EC_e calibration. From this information, modifications were made to the current protocols and guidelines developed by Corwin and Lesch (2013) to specifically address EC_a surveys of fields under micro-irrigation.

2.1. Site description

A pistachio orchard on Flores Farm located near Lemoore, CA (36.3008° N, 119.7829° W, elevation of 72 m above sea level) in Kings County was selected as the study site (Fig. 3). Flores pistachio orchard resides in the southern region of California's San Joaquin Valley, which has a Mediterranean climate with rainfall occurring primarily during winter months (November through February). The orchard consists of pistachio trees of Kerman cultivar grafted onto Pioneer Gold 1 (PG1) rootstock and is drip irrigated with dual drip lines. Site selection was based on obtaining an orchard that contained mature trees with well-developed root systems under drip irrigation for a decade or more, which would result in a spatial distribution of soil salinity within the root zone resembling that of Fig. 1. The Flores Farm pistachio orchard, a 57-ha block, has mature trees planted during the late 1980s at a 5 m x 5 m spacing on a Lethent clay loam soil.

The micro-irrigation system consists of dual drip lines with eight Netafim Triton X pressure-compensating drippers per tree with nominal flowrate of 1.9 L h^{-1}. The actual system application rate is 0.43 mm h^{-1} with average emitters' flowrate of 1.4 L h^{-1}. The irrigation water applied by growers was measured and recorded using magnetic flowmeters (Sensus iPEARL, Raleigh, NC, USA). Irrigation water was applied every 2–3 days on average, and about 250–400 mm was applied. Part of this water was applied before leaf-out to refill the soil profile and part was applied from leaf-out to meet the ET and leaching requirements during that period. Soil moisture was monitored by means of granular matrix moisture tension sensors (Watermark, Irrometer Company, Inc., Riverside, CA, USA) installed at the depths of 0.40 m, 0.90 m, and 1.20 m. The farm manager scheduled irrigation based on a combination of ET and soil moisture and maintained the moisture tension in the root zone consistently above − 50 kPa.

Two subsections within the Flores pistachio orchard designated D01 and D05 were selected to provide a range of soil salinities and sodic conditions. Subsection D01 was 230 m x 200 m and D05 was 200 m x 200 m. Preliminary data collected from an EC_a-directed soil sampling of the Flores orchard indicated that subsection D01 ranged in salinity (i.e., EC_e) from 2 to 13.3 dS m^{-1}, sodium adsorption ratio (SAR) from 7 to 43, and pH_e from 7.4 to 7.8. Subsection D05 ranged in salinity (i.e., EC_e) from 2 to 13 dS m^{-1}, SAR from 3 to 40, and pH_e from 7.4 to 7.8. The ranges and standard deviations of EC_e and SAR for D01 and D05 indicate that there was variation in salinity and sodium levels for both subsections.

2.2. EC_a-directed soil sampling survey

The field-scale distribution of soil salinity was assessed following the EC_a-directed soil sampling protocols and guidelines of Corwin and Lesch (2003, 2005b, 2013) and summarized by Corwin and Scudiero (2020). All measurements of EC_a were taken using a Geonics[1] dual-dipole EM38 electromagnetic conductivity meter (Geonics Limited, Mississauga, Ontario, Canada).

EC_a surveys were conducted using a mobile cart pulled by hand with the electromagnetic induction (EMI) and coupled GPS equipment secured to the cart. Ten equally spaced traverses (20 m apart) were taken with the electromagnetic conductivity meter within each of the Flores (D01 and D05) sites. Along each traverse EC_a measurements were taken every 3–5 m. Measurements of EC_a were taken in the horizontal (EM_h) and vertical (EM_v) dipole modes to provide shallow (0–0.75 m) and deep (0–1.5 m) measurements of EC_a, respectively. The EC_a measurement locations were georeferenced with sub-meter accuracy using a Trimble[1] Pro-XRS GPS system (Trimble, Sunnyvale, CA, USA). Flores

[1] All references to commercial equipment and instrumentation are provided solely for the benefit of the reader and do not imply the endorsement of the USDA-ARS.

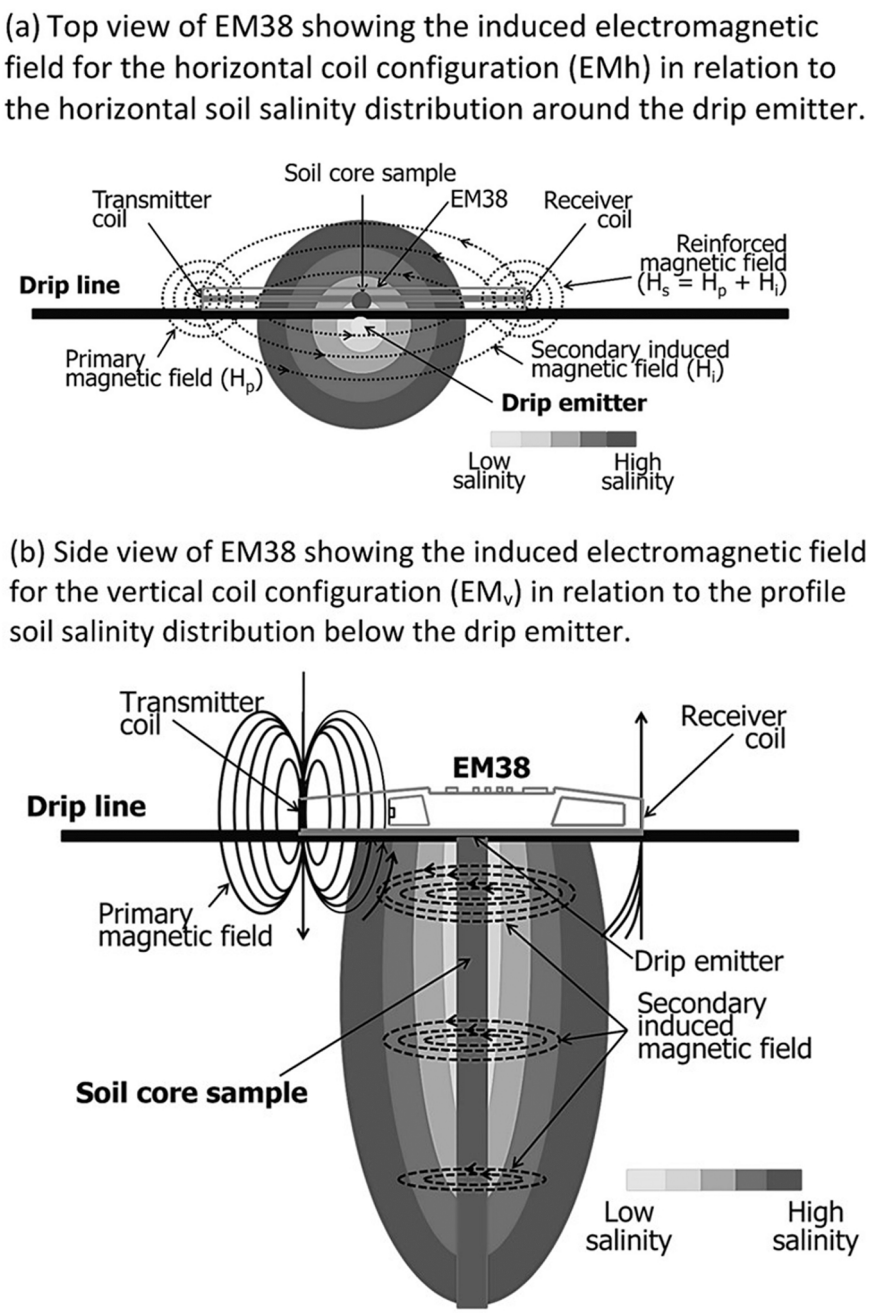

Fig. 2. Top (a) and profile (b) views showing the association of idealized soil salinity distribution, electromagnetic induction primary and secondary induced magnetic fields, and soil sample location as selected according to the Corwin and Lesch (2013) EC_a-directed soil sampling protocols.

D01 and D05 were surveyed in March 2018. The EC_a surveys of EM_v and EM_h for Flores D01 and D05 are provided in Fig. 4.

2.3. Soil sampling design

Using the EC_a survey data and ESAP software (Lesch et al., 2000), 12 initial soil core sampling locations were selected at each site (i.e., Flores D01 and Flores D05) to represent the frequency distribution of the bivariate EMI survey data for each site, and to be allocated across each site to avoid spatial clustering (Fig. 4a, b). Soil cores were taken in the days following the EC_a surveys.

The initial 12 soil core locations (24 soil core locations total) taken within each of the Flores sites (D01 and D05) were used to characterize the field-scale variation in soil properties and to determine the robustness of the EC_a-directed soil sampling protocols in developing a reliable EC_a – EC_e calibration at each site. Soil samples at the 12 locations in D01 and 12 locations in D05 were taken at 0.3-m depth increments (i.e., 0–0.3, 0.3–0.6, 0.6–0.9, 0.9–1.2, and 1.2–1.5 m) to a depth of 1.5 m, resulting in 60 core samples at each site (120 total samples). The soil cores were taken at the drip line near the tree trunk. Additional soil cores were taken at 6 of the 12 locations within both D01 and D05 (see circled locations in Fig. 4), which were used to characterize local-scale variation and to determine the best soil core location or combination of soil core locations to produce the most reliable EC_a – EC_e calibration. The additional soil cores consisted of cores taken at 0, 0.3, 0.6, 0.9, 1.2, and 1.5 m perpendicular to the drip line at 0.3-m depth increments down to 1.5 m. These 6 soil core positions at and perpendicular to the drip line are designated as L_0, L_1, L_2, L_3, L_4, and L_5, corresponding to the distances of 0, 0.3, 0.6, 0.9, 1.2, and 1.5 m perpendicular to the drip line, respectively (Fig. 5). All soil cores were kept in refrigerated storage prior to air-

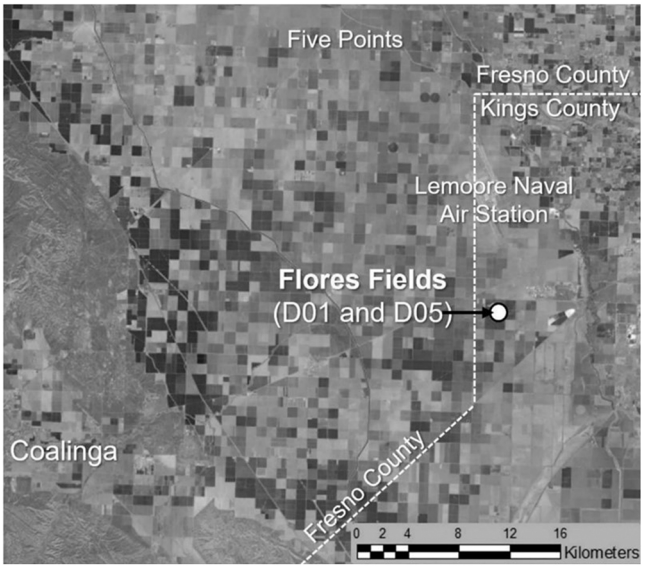

Fig. 3. Aerial photograph of the location of Flores Farm orchard near Lemoore, CA.

drying and sieving (2-mm sieve), which occurred within a few days after their collection. Soil samples were analyzed for EC_e, SP, SAR, gravimetric water content at field capacity (θ_g), and pH_e following the chemical analysis procedures presented in *Methods of Soil Analysis* (Sparks, 1996).

The decision to sample out to 1.5 m perpendicular to the drip line from the tree is based on an accepted rule-of-thumb that the radius of the root system for a tree crop is approximately equal to the radius of the canopy. The average radius of the pistachio canopy in D01 and D05 was approximately 1.5 m. The decision to sample to a depth of 1.5 m is based on the depth of measurement of the EM38, which is approximately 1.5 m. The soil core sample design resulted in 180 soil core samples for D01 and 180 for D05 (i.e., 6 locations x 6 positions perpendicular to the drip line x 5 depth increments = 180). This intensive soil sampling also provided a means of estimating the volume of measurement of both the EM_h and EM_v coil configurations by determining the collection of soil samples whose combined EC_e best correlated with EM_h EC_a and EM_v EC_a.

3. Results and discussion

Maps of SP and EC_e for the top 0–1.5 m of soil for D01 and D05 are shown in Fig. 6a and 6b, respectively. These maps show the field-scale variation in these soil properties at the drip lines since the soil samples were taken only in the drip line at all 12 locations within each subsection (i.e., D01 and D05). The soil profiles below the drip lines reflect the lowest salinity levels and highest water contents, which subsequently provide a biased, optimistic view of the salinity affecting the pistachio yield. The maps of Fig. 6 provide only general spatial trends in soil properties at field scale that are extremely biased and are most likely of extremely limited value from a salinity management perspective.

3.1. Analysis of soil profile salinity data

To evaluate the influence of local-scale salinity gradients resulting from drip irrigation on EC_a measurements with the EM38, it was important to determine whether local-scale salinity gradients like those depicted in Fig. 1 existed at the two selected sites (i.e., D01 and D05). Figs. 7 and 8 show graphs of the salinity profiles for L_0, L_1, L_2, L_3, L_4, and L_5 for the Flores D01 and Flores D05 sites, respectively, where the EC_e is the average for a depth increment of the 6 intensively sampled locations for a given core. Figs. 7 and 8 indicate that a local-scale gradient of salinity exists within the root zone across both D01 and D05 due to a decade or more of drip irrigation. At both sites the general trend is for soil salinity to increase as the distance increases from the drip line and for salinity to increase with depth. These figures provide a realistic view of the local-scale root zone salinity affecting pistachio yield at D01 and D05.

Calculation of the average absolute difference (AAD) between the average salinity profile and each of the salinity profiles for positions L_0, L_1, L_2, L_3, L_4, and L_5 provides a means of determining which of the soil cores comes closest to the average salinity profile of the 6 soil cores (i.e., L_0, L_1, L_2, L_3, L_4, and L_5). The average absolute difference is shown in Eq. (1):

$$AAD_{L_p} = \frac{1}{n}\sum_{i=1}^{n}\left|\overline{EC_{e,n}} - EC_{e,L_{p,n}}\right| \quad (1)$$

where p is 0, 1, 2, 3, 4, or 5 and corresponds to the positions where soil cores were taken at L_0, L_1, L_2, L_3, L_4, and L_5, respectively, n is the depth increment (i.e., $n = 1$ is 0–0.3 m, $n = 2$ is 0.3–0.6 m, $n = 3$ is 0.6–0.9 m, $n = 4$ is 0.9–1.2 m, and $n = 5$ is 1.2–1.5 m), $\overline{EC_{e,n}}$ is the average EC_e of L_0, L_1, L_2, L_3, L_4, and L_5 at depth n, and EC_{e,L_n} is the EC_e at depth n for position L_0, L_1, L_2, L_3, L_4, or L_5. The average soil profile salinity for D01 lies closest to L_4, which is the soil core taken at 1.2 m from the drip line, and for D05 lies closest to L_2 taken at 0.6 m from the drip line. Ostensibly, this suggests that taking a soil core between 0.6 and 1.2 m (between L_2 and L_4) from the drip line provides a better representation of the average soil salinity than from below the drip line at L_0. In both D01 and D05 the average soil profile salinity fell between L_2 (0.6 m) and L_4 (1.2 m). However, the lowest AAD occurs when L_2 and L_4 are averaged, suggesting that the average salinity profile within the root zone of a pistachio tree in D01 and D05 might be estimated by averaging soil cores taken at positions L_2 and L_4, which are 0.6 m and 1.2 m, respectively, from the drip line under the tree canopy. L_2 and L_4 correspond to approximately 40% and 80% of the radius of the canopy in D01 and D05.

Characterizing the average root zone salinity under drip irrigation may be useful in the calibration of EC_a to EC_e since EC_a measurements with the EM38 encompass a sphere of measurement of approximately 1–2 m^3, which comprises a substantial portion of the root system where salinity varies considerably both horizontally and vertically. Establishing the best location to take a soil core or combination of cores to characterize the corresponding volume of measurement of the EM38 when drip irrigation has created significant gradients in salinity is a knowledge gap in current EC_a-directed soil sampling protocols that needs to be filled. However, using Eq. (1) to determine where to take a soil core sample may be problematic because it assumes that the best reflection of the volume of measurement by the EM38 is the average salinity profile, which may or may not be true.

To better understand how the EC_a – EC_e calibration benefits from a well-positioned soil core sample or combination of coil samples, simple correlations between EC_a (both EM_h and EM_v) and EC_e were calculated where EC_e was determined over various composite depths and composites of soil cores, including L_0 alone, which is the soil core location recommended by the current protocols of Corwin and Lesch (2013). The highest correlation coefficient would reflect the soil core best to represent the volume of measurement of the EM38.

3.1.1. Flores D01 site

Table 1 is a compilation of the correlation coefficients between EMh ECa and ECe and between EMv ECa and ECe for various composites of soil cores (i.e., L0, L0 + L1, L0 + L1 + L2, L0 + L1 + L2 + L3, L0 + L1 + L2 + L3 + L4, and L0 + L1 + L2 + L3 + L4 + L5). The lowest correlation for D01 for both EMh and EMv predominantly occurred when ECe was measured solely from soil core L0 at all composite depth increments. The highest correlation for D01 for both EMh and EMv

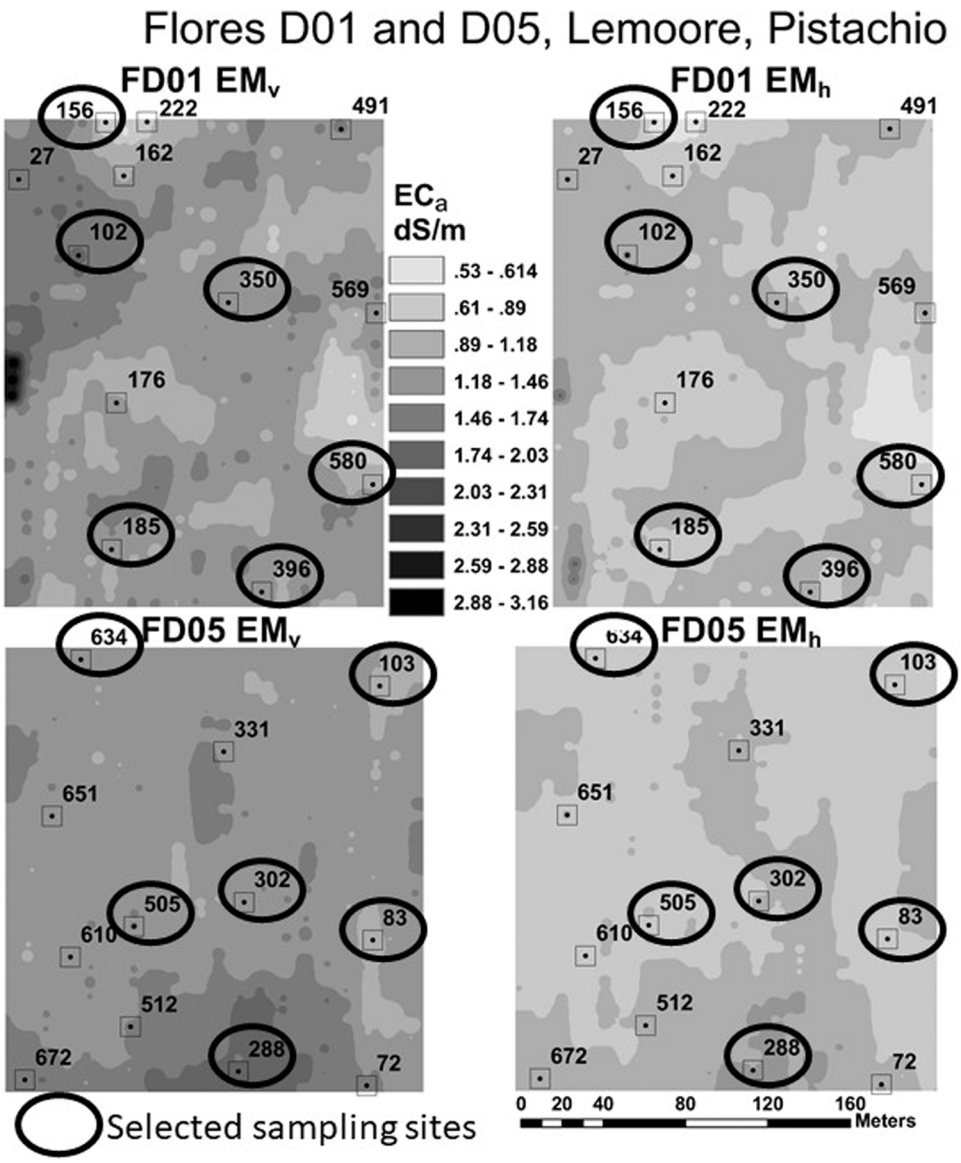

Fig. 4. Apparent soil electrical conductivity (EC_a, dS m^{-1}) surveys measured with electromagnetic induction in the vertical coil configuration (EM_v) and in the horizontal coil configuration (EM_h) at (a and b) Flores D01 and (c and d) Flores D05 field sites. Squares indicate the 12 soil core locations identified using ESAP software where single soil cores in the drip line were taken at 0.3-m depth increments to a depth of 1.5 m. Circled squares indicate 6 of the 12 soil core locations in the Flores D01 and D05 sites where 6 soil cores were taken at 0, 0.3, 0.6, 0.9, 1.2, and 1.5 m perpendicular to the drip line at 0.3-m depth increments down to 1.5 m.

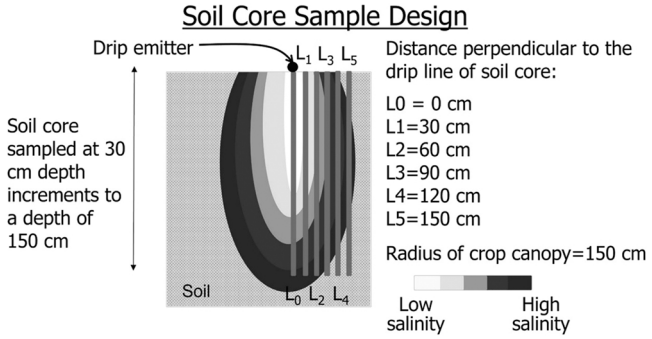

Fig. 5. Soil core sample design for the intensively sampled sites at both D01 and D05, showing the location of the 6 soil cores at 0, 0.3, 0.6, 0.9, 1.2, and 1.5 m perpendicular to the drip line, which are designated as L_0, L_1, L_2, L_3, L_4, and L_5, respectively.

occurred when ECe was measured for a composite of all 6 soil core positions (i.e., L0 +L1 +L2 +L3 +L4 +L5) and averaged, with correlation coefficients (r) of 0.72 for EMh and 0.65 for EMv. The highest correlations occur for the composite depth of 0–1.2 m for EMh and 0–1.5 m for EMv, which reflects the depth of penetration of EMh and EMv. This suggests that a better measure of ECe is obtained for the volume of measurement of ECa by the EM38 when all soil cores were combined providing a better average measurement of the salinity gradient across the instrument's volume of measurement. Theoretically, the EM38 has a depth of measurement for EMh ECa of 0.5–0.75 m and for the EMv ECa of 1.2–1.5 m, which is the 'skin depth' (i.e., depth at which the EM38 signal is attenuated by 1/e). However, as pointed out above, one means of estimating the actual depth of measurement in the field is to determine the composite depth increment that results in the highest correlation coefficient (Corwin and Lesch, 2013). The actual depth of measurement may be different from the theoretical 'skin depth' (Corwin and Lesch, 2013).

There was also a correlation between EC_a and SP at D01 (Table 2). A correlation between EC_a and more than one edaphic property is common since EC_a is influenced by salinity, water content, bulk density, and texture (Corwin and Lesch, 2003, 2005b). Saturation percentage is a reflection of the soil texture. High correlations were found between EC_a and SP for both EM_h EC_a and EM_v EC_a at all soil core composites (i.e., L_0, $L_0 + L_1$, $L_0 + L_1 + L_2$, $L_0 + L_1 + L_2 + L_3$, $L_0 + L_1 + L_2 + L_3 + L_4$, and $L_0 + L_1 + L_2 + L_3 + L_4 + L_5$). The high correlations for all soil core composites is expected since texture does not have high local-scale

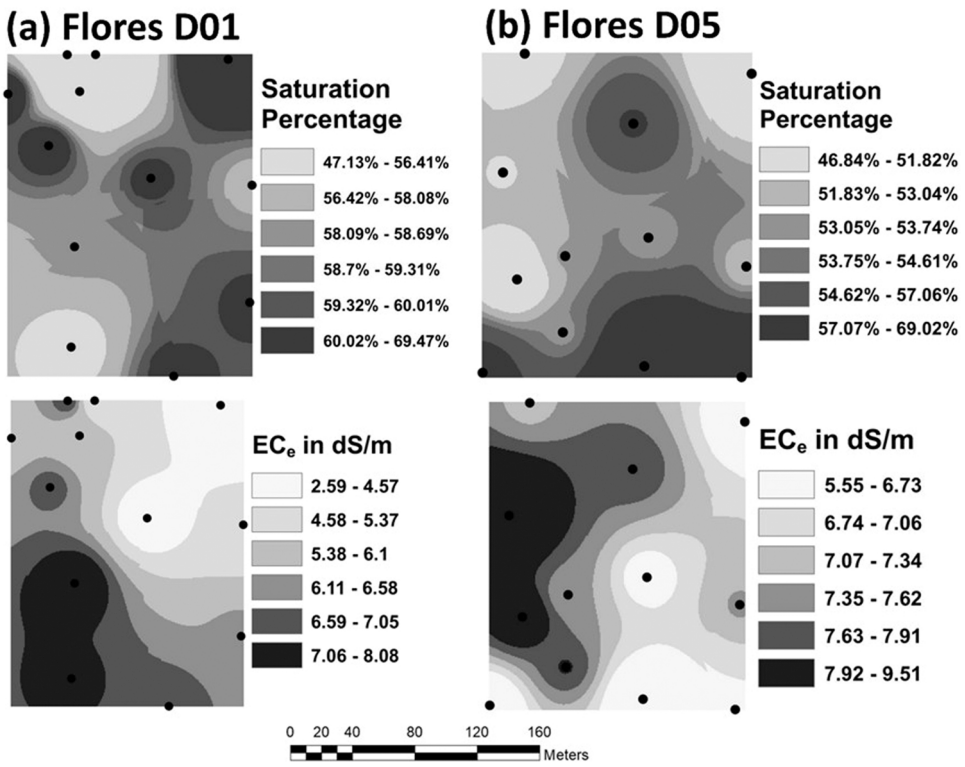

Fig. 6. Interpolated maps of electrical conductivity of the saturation extract (EC_e, dS m^{-1}) and saturation percentage (SP) for the composite 0–1.5 m depth increment using the 12 soil cores in each of the (a) Flores D01 and (b) Flores D05 sites.

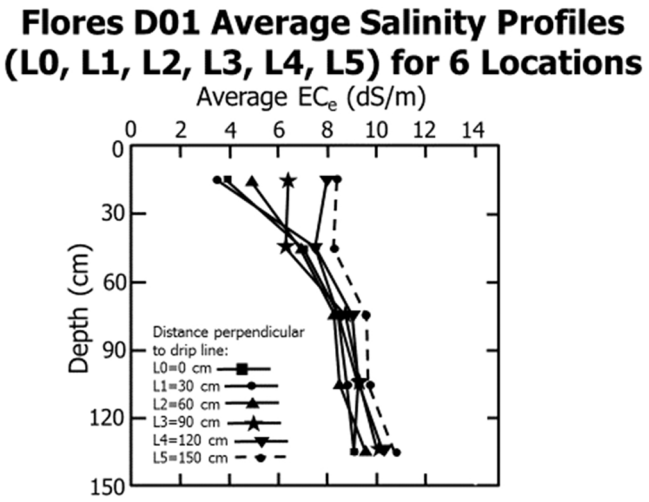

Fig. 7. Graph of the salinity profiles for L_0, L_1, L_2, L_3, L_4, and L_5 for the Flores D01 site with EC_e (electrical conductivity of the saturation extract, dS m^{-1}) vs soil depth where the EC_e is the average for a depth increment of the 6 intensively sampled locations for a given core.

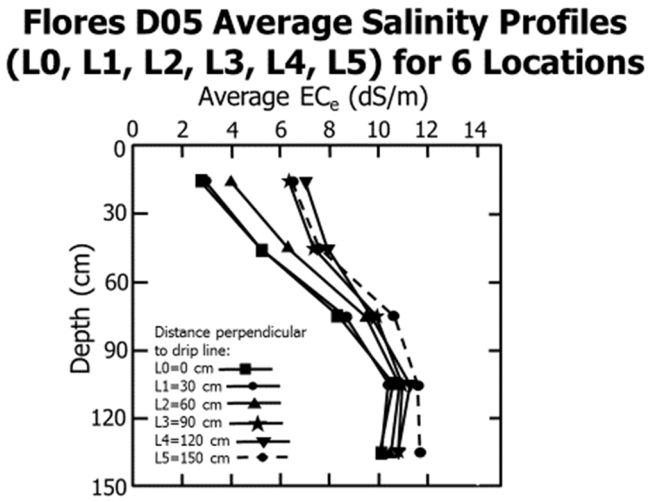

Fig. 8. Graph of the salinity profiles for L_0, L_1, L_2, L_3, L_4, and L_5 for the Flores D05 site with EC_e (electrical conductivity of the saturation extract, dS m^{-1}) vs soil depth where the EC_e is the average at a depth increment of the 6 locations for a given core.

variability. As was the case in Table 1, Table 2 shows the highest correlation for the composite depth of 0–1.2 m for EM_h and 0–1.5 m for EM_v.

Table 3 establishes the single core that best approximates the salinity gradients measured within the volume of measurement of the EM38. The correlation coefficients for L_3 and L_4 soil cores, corresponding to 0.9 and 1.2 m from the drip line, are the highest and are similar in value at a composite depth of 0–0.9 m for EM_h EC_a ($r = 0.79$ and $r = 0.79$, respectively) and a composite depth of 0–1.5 m for EM_v EC_a ($r = 0.78$ and $r = 0.79$, respectively). Table 4 shows the best combination of two soil cores that approximates the salinity gradients measured within the volume of measurement of the EM38. The combination of soil cores $L_0 + L_5$ have the highest correlation coefficients for both EM_h and EM_v ($r = 0.77$ and $r = 0.71$, respectively). Not shown in Table 4 is the high correlation coefficient of the combination of soil cores $L_3 + L_4$, which had high correlation coefficients, but not quite as high as $L_0 + L_5$. The composite depth with the highest correlation coefficient was 0–0.9 m for EM_h and 0–1.5 m for EM_v. For Tables 1–4 the highest correlations between EM_h EC_a and EC_e were for composite soil cores of either 0–0.9 m or 0–1.2 depth, suggesting the actual depth may be around 1 m, which is

Table 1
Correlation coefficients between (a) EM_h and EC_e and (b) EM_v and EC_e for various soil core combinations at depths of 0–30, 0–60, 0–90, 0–120, and 0–150 cm taken at site Flores D01. 'Current protocols' refers to the protocols presented by Corwin and Lesch (2013) for apparent soil electrical conductivity (EC_a) directed soil sampling of drip irrigated fields, which calibrates EC_a to EC_e using a single soil core taken from directly below the drip line (i.e., L_0).

(a) Flores D01: Correlation coefficient between EM_h and EC_e

Depth (cm)	L_0 (current protocols)	$L_0 + L_1$	$L_0 + L_1 + L_2$	$L_0 + L_1 + L_2 + L_3$	$L_0 + L_1 + L_2 + L_3 + L_4$	$L_0 + L_1 + L_2 + L_3 + L_4 + L_5$
0–30	0.032	0.018	0.132	0.098	0.105	0.194
0–60	0.095	0.132	0.127	0.153	0.185	0.199
0–90	0.338	0.337	0.339	0.367	0.410	0.446
0–120	0.495	0.455	0.467	0.460	0.692	**0.718**
0–150	0.474	0.487	0.431	0.442	0.658	0.694

(b) Flores D01: Correlation coefficient between EM_v and EC_e

Depth (cm)	L_0 (current protocols)	$L_0 + L_1$	$L_0 + L_1 + L_2$	$L_0 + L_1 + L_2 + L_3$	$L_0 + L_1 + L_2 + L_3 + L_4$	$L_0 + L_1 + L_2 + L_3 + L_4 + L_5$
0–30	0.145	0.404	0.344	0.301	0.300	0.384
0–60	0.069	0.168	0.205	0.236	0.261	0.257
0–90	0.342	0.376	0.396	0.416	0.451	0.475
0–120	0.448	0.512	0.497	0.483	0.463	0.556
0–150	0.453	0.593	0.518	0.502	0.597	**0.647**

L_0 is the soil core location 0 cm perpendicular to the drip line, L_1 is 0.3 m perpendicular to the drip line, L_2 is 0.6 m, L_3 is 0.9 m, L_4 is 1.2 m, and L_5 is 1.5 m perpendicular to the drip line. $L_0 + L_1$ is the combination of soil cores L_0 and L_1; $L_0 + L_1 + L_2$ is the combination of sol cores L_0, L_1, and L_2; and so forth. Bold type indicates the highest correlation coefficient. EM_h refers to the measurement of EC_a in the horizontal coil configuration (dS m^{-1}). EM_v refers to the measurement of EC_a in the horizontal coil configuration (dS m^{-1}). EC_e refers to the electrical conductivity of the saturation extract (dS m^{-1}).

somewhat surprising since the theoretical 'skin' depth is 0.5–0.75 m. However, the actual depth of measurement of EM_h EC_a and EM_v EC_a may not always equal the theoretical 'skin' depth as found by Corwin and Lesch (2013).

3.1.2. Flores D05 site

Table 5 indicates the highest correlation coefficient for D05 for both EM_h and EM_v occurred when EC_e was a composite of the 0–0.9 m soil core depth for EM_h and composite depth of 0–1.5 m for EM_v and all 6 soil core positions were combined (i.e., $L_0 + L_1 + L_2 + L_3 + L_4 + L_5$) and averaged with correlation coefficients (r) of 0.79 for EM_h and 0.75 for EM_v (Table 5). Similar to D01, strong correlations between EC_a and SP were found for all combinations of soil cores (i.e., L_0, $L_0 + L_1$, $L_0 + L_1 + L_2$, $L_0 + L_1 + L_2 + L_3$, $L_0 + L_1 + L_2 + L_3 + L_4$, and $L_0 + L_1 + L_2 + L_3 + L_4 + L_5$) for both EM_h and EM_v indicating the low local-scale variability of soil texture (Table 6). The correlation of EC_a to EC_e using a single soil core worked best with the L_4 core position (1.2 m from the drip line) for D05, with r of 0.78 for EM_h and 0.79 for EM_v (Table 7). Table 8 shows the best combination of two soil cores that approximates the salinity gradients measured within the volume of measurement of the EM38. The combination of soil cores $L_0 + L_5$ have the highest correlation coefficients for both EM_h and EM_v ($r = 0.78$ and $r = 0.74$, respectively). Not shown in Table 8 is the high correlation coefficient of the combination of soil cores $L_2 + L_4$, which had comparable correlation coefficients of $r = 0.76$ and $r = 0.77$, respectively, for EM_h and EM_v. From Tables 4–8 the depth of measurement was either 0–0.90 m or 0–1.2 m for EM_h and was consistently 0–1.5 m for EM_v.

Table 2
Correlation coefficients between (a) EM_h and SP and (b) EM_v and SP for various soil core combinations at depths of 0–30, 0–60, 0–90, 0–120, and 0–150 cm taken at site Flores D01. 'Current protocols' refers to the protocols presented by Corwin and Lesch (2013) for apparent soil electrical conductivity (EC_a) directed soil sampling of drip irrigated fields, which calibrates EC_a to SP using a single soil core taken from directly below the drip line (i.e., L_0).

(a) Flores D01: Correlation coefficient between EM_h and SP

Depth (cm)	L_0 (current protocols)	$L_0 + L_1$	$L_0 + L_1 + L_2$	$L_0 + L_1 + L_2 + L_3$	$L_0 + L_1 + L_2 + L_3 + L_4$	$L_0 + L_1 + L_2 + L_3 + L_4 + L_5$
0–30	0.136	0.217	0.173	0.246	0.421	0.063
0–60	0.548	0.430	0.282	0.268	0.322	0.369
0–90	0.677	0.487	0.411	0.483	0.543	0.636
0–120	**0.772**	**0.692**	**0.672**	**0.670**	**0.647**	**0.712**
0–150	0.405	0.378	0.359	0.360	0.311	0.343

(b) Flores D01: Correlation coefficient between EM_v and SP

Depth (cm)	L_0 (current protocols)	$L_0 + L_1$	$L_0 + L_1 + L_2$	$L_0 + L_1 + L_2 + L_3$	$L_0 + L_1 + L_2 + L_3 + L_4$	$L_0 + L_1 + L_2 + L_3 + L_4 + L_5$
0–30	0.069	0.067	0.137	0.143	0.364	0.000
0–60	0.303	0.257	0.221	0.184	0.136	0.187
0–90	0.363	0.332	0.208	0.177	0.181	0.185
0–120	0.452	0.497	0.426	0.482	0.529	0.593
0–150	**0.636**	**0.650**	**0.534**	**0.675**	**0.692**	**0.723**

L_0 is the soil core location 0 cm perpendicular to the drip line, L_1 is 0.3 m perpendicular to the drip line, L_2 is 0.6 m, L_3 is 0.9 m, L_4 is 1.2 m, and L_5 is 1.5 m perpendicular to the drip line. $L_0 + L_1$ is the combination of soil cores L_0 and L_1; $L_0 + L_1 + L_2$ is the combination of sol cores L_0, L_1, and L_2; and so forth. Bold type indicates the highest correlation coefficient at a given depth. EM_h refers to the measurement of EC_a in the horizontal coil configuration (dS m^{-1}). EM_v refers to the measurement of EC_a in the horizontal coil configuration (dS m^{-1}). SP refers to the saturation percentage.

Table 3
Correlation coefficients between (a) EM_h and EC_e and (b) EM_v and EC_e for various soil cores (i.e., L_0, L_1, L_2, L_3, L_4, and L_5) at depths of 0–30, 0–60, 0–90, 0–120, and 0–150 cm taken at site Flores D01. 'Current protocols' refers to the protocols presented by Corwin and Lesch (2013) for apparent soil electrical conductivity (EC_a) directed soil sampling of drip irrigated fields, which calibrates EC_a to EC_e using a single soil core taken from directly below the drip line (i.e., L_0).

(a) Flores D01: Correlation coefficient between EM_h and EC_e

Depth (cm)	L_0 (current protocols)	L_1	L_2	L_3	L_4	L_5
0–30	0.032	0.111	0.290	0.221	0.328	0.273
0–60	0.095	0.188	0.256	0.333	0.359	0.195
0–90	0.338	0.329	0.413	**0.791**	**0.794**	0.566
0–120	0.495	0.444	0.475	0.728	0.768	0.595
0–150	0.474	0.481	0.523	0.649	0.646	0.547

(b) Flores D01: Correlation coefficient between EM_v and EC_e

Depth (cm)	L_0 (current protocols)	L_1	L_2	L_3	L_4	L_5
0–30	0.145	0.391	0.452	0.342	0.443	0.387
0–60	0.069	0.186	0.307	0.306	0.307	0.293
0–90	0.342	0.353	0.431	0.522	0.601	0.566
0–120	0.448	0.502	0.507	0.579	0.598	0.540
0–150	0.453	0.541	0.553	**0.777**	**0.789**	0.569

L_0 is the soil core location 0 cm perpendicular to the drip line, L_1 is 0.3 m perpendicular to the drip line, L_2 is 0.6 m, L_3 is 0.9 m, L_4 is 1.2 m, and L_5 is 1.5 m perpendicular to the drip line. Bold type indicates the highest correlation coefficient at a given depth. EM_h refers to the measurement of EC_a in the horizontal coil configuration (dS m^{-1}). EM_v refers to the measurement of EC_a in the horizontal coil configuration (dS m^{-1}). EC_e refers to the electrical conductivity of the saturation extract (dS m^{-1}).

Table 4
Correlation coefficients between (a) EM_h and EC_e and (b) EM_v and EC_e for various soil core combinations (i.e., $L_0 + L_1$, $L_0 + L_2$, $L_0 + L_3$, $L_0 + L_4$, and $L_0 + L_5$) at depths of 0–30, 0–60, 0–90, 0–120, and 0–150 cm taken at site Flores D01. 'Current protocols' refers to the protocols presented by Corwin and Lesch (2013) for apparent soil electrical conductivity (EC_a) directed soil sampling of drip irrigated fields, which calibrates EC_a to EC_e using a single soil core taken from directly below the drip line (i.e., L_0).

(a) Flores D01: Correlation coefficient between EM_h and EC_e

Depth (cm)	L_0 (current protocols)	$L_0 + L_1$	$L_0 + L_2$	$L_0 + L_3$	$L_0 + L_4$	$L_0 + L_5$
0–30	0.032	0.018	0.301	0.259	0.203	0.349
0–60	0.095	0.132	0.247	0.155	0.350	0.359
0–90	0.338	0.337	0.431	0.553	0.591	**0.774**
0–120	0.495	0.455	0.499	0.495	0.542	0.776
0–150	0.474	0.487	0.544	0.531	0.729	0.697

(b) Flores D01: Correlation coefficient between EM_v and EC_e

Depth (cm)	L_0 (current protocols)	$L_0 + L_1$	$L_0 + L_2$	$L_0 + L_3$	$L_0 + L_4$	$L_0 + L_5$
0–30	0.145	0.404	0.473	0.371	0.359	0.478
0–60	0.069	0.168	0.315	0.203	0.356	0.215
0–90	0.342	0.376	0.457	0.563	0.592	0.688
0–120	0.448	0.512	0.511	0.475	0.477	0.557
0–150	0.453	0.593	0.519	0.460	0.647	**0.711**

L_0 is the soil core location 0 cm perpendicular to the drip line, L_1 is 0.3 m perpendicular to the drip line, L_2 is 0.6 m, L_3 is 0.9 m, L_4 is 1.2 m, and L_5 is 1.5 m perpendicular to the drip line. Bold type indicates the highest correlation coefficient at a given depth. EM_h refers to the measurement of EC_a in the horizontal coil configuration (dS m^{-1}). EM_v refers to the measurement of EC_a in the horizontal coil configuration (dS m^{-1}). EC_e refers to the electrical conductivity of the saturation extract (dS m^{-1}).

Table 5
Correlation coefficients between (a) EM_h and EC_e and (b) EM_v and EC_e for various soil core combinations at depths of 0–30, 0–60, 0–90, 0–120, and 0–150 cm taken at site Flores D01. 'Current protocols' refers to the protocols presented by Corwin and Lesch (2013) for apparent soil electrical conductivity (EC_a) directed soil sampling of drip irrigated fields, which calibrates EC_a to EC_e using a single soil core taken from directly below the drip line (i.e., L_0).

(a) Flores D05: Correlation coefficient between EM_h and EC_e

Depth (cm)	L_0 (current protocols)	$L_0 + L_1$	$L_0 + L_1 + L_2$	$L_0 + L_1 + L_2 + L_3$	$L_0 + L_1 + L_2 + L_3 + L_4$	$L_0 + L_1 + L_2 + L_3 + L_4 + L_5$
0–30	0.269	0.370	0.203	0.589	0.520	0.250
0–60	0.271	0.293	0.215	0.670	0.729	0.580
0–90	0.404	0.475	0.533	0.776	0.779	**0.794**
0–120	0.379	0.434	0.420	0.668	0.769	0.768
0–150	0.242	0.310	0.336	0.359	0.304	0.314

(b) Flores D05: Correlation coefficient between EM_v and EC_e

Depth (cm)	L_0 (current protocols)	$L_0 + L_1$	$L_0 + L_1 + L_2$	$L_0 + L_1 + L_2 + L_3$	$L_0 + L_1 + L_2 + L_3 + L_4$	$L_0 + L_1 + L_2 + L_3 + L_4 + L_5$
0–30	0.264	0.270	0.219	0.286	0.238	0.265
0–60	0.208	0.226	0.460	0.403	0.554	0.589
0–90	0.335	0.525	0.537	0.449	0.582	0.501
0–120	0.373	0.572	0.564	0.524	0.593	0.597
0–150	0.411	0.541	0.522	0.534	0.661	**0.751**

L_0 is the soil core location 0 cm perpendicular to the drip line, L_1 is 0.3 m perpendicular to the drip line, L_2 is 0.6 m, L_3 is 0.9 m, L_4 is 1.2 m, and L_5 is 1.5 m perpendicular to the drip line. $L_0 + L_1$ is the combination of soil cores L_0 and L_1; $L_0 + L_1 + L_2$ is the combination of sol cores L_0, L_1, and L_2; and so forth. Bold type indicates the highest correlation coefficient. EM_h refers to the measurement of EC_a in the horizontal coil configuration (dS m^{-1}). EM_v refers to the measurement of EC_a in the horizontal coil configuration (dS m^{-1}). EC_e refers to the electrical conductivity of the saturation extract (dS m^{-1}).

Table 6
Correlation coefficients between (a) EM_h and SP and (b) EM_v and SP for various soil core combinations at depths of 0–30, 0–60, 0–90, 0–120, and 0–150 cm taken at site Flores D01. 'Current protocols' refers to the protocols presented by Corwin and Lesch (2013) for apparent soil electrical conductivity (EC_a) directed soil sampling of drip irrigated fields, which calibrates EC_a to SP using a single soil core taken from directly below the drip line (i.e., L_0).

(a) Flores D05: Correlation coefficient between EM_h and SP

Depth (cm)	L_0 (current protocols)	$L_0 + L_1$	$L_0 + L_1 + L_2$	$L_0 + L_1 + L_2 + L_3$	$L_0 + L_1 + L_2 + L_3 + L_4$	$L_0 + L_1 + L_2 + L_3 + L_4 + L_5$
0–30	0.837	0.856	0.866	0.879	0.849	0.787
0–60	0.927	0.918	0.916	0.909	0.913	0.811
0–90	0.823	0.714	0.574	0.403	0.296	0.106
0–120	**0.794**	**0.925**	**0.962**	**0.939**	**0.958**	**0.955**
0–150	0.578	0.409	0.149	0.143	0.260	0.199

(b) Flores D05: Correlation coefficient between EM_v and SP

Depth (cm)	L_0 (current protocols)	$L_0 + L_1$	$L_0 + L_1 + L_2$	$L_0 + L_1 + L_2 + L_3$	$L_0 + L_1 + L_2 + L_3 + L_4$	$L_0 + L_1 + L_2 + L_3 + L_4 + L_5$
0–30	0.802	0.788	0.734	0.738	0.593	0.520
0–60	0.526	0.533	0.572	0.578	0.646	0.622
0–90	0.593	0.596	0.587	0.561	0.596	0.569
0–120	0.535	0.535	0.755	0.664	0.602	0.528
0–150	**0.800**	**0.741**	**0.737**	**0.741**	**0.745**	**0.735**

L_0 is the soil core location 0 cm perpendicular to the drip line, L_1 is 0.3 m perpendicular to the drip line, L_2 is 0.6 m, L_3 is 0.9 m, L_4 is 1.2 m, and L_5 is 1.5 m perpendicular to the drip line. $L_0 + L_1$ is the combination of soil cores L_0 and L_1; $L_0 + L_1 + L_2$ is the combination of sol cores L_0, L_1, and L_2; and so forth. Bold type indicates the highest correlation coefficient at a given depth. EM_h refers to the measurement of EC_a in the horizontal coil configuration (dS m^{-1}). EM_v refers to the measurement of EC_a in the horizontal coil configuration (dS m^{-1}). SP refers to the saturation percentage.

Table 7
Correlation coefficients between (a) EM_h and EC_e and (b) EM_v and EC_e for various soil cores (i.e., L_0, L_1, L_2, L_3, L_4, and L_5) at depths of 0–30, 0–60, 0–90, 0–120, and 0–150 cm taken at site Flores D01. 'Current protocols' refers to the protocols presented by Corwin and Lesch (2013) for apparent soil electrical conductivity (EC_a) directed soil sampling of drip irrigated fields, which calibrates EC_a to EC_e using a single soil core taken from directly below the drip line (i.e., L_0).

(a) Flores D05: Correlation coefficient between EM_h and EC_e

Depth (cm)	L_0 (current protocols)	L_1	L_2	L_3	L_4	L_5
0–30	0.269	0.312	0.293	0.571	0.528	0.271
0–60	0.271	0.388	0.246	0.663	0.719	0.591
0–90	0.404	0.421	0.533	0.681	**0.783**	0.666
0–120	0.379	0.454	0.457	0.682	0.696	0.595
0–150	0.242	0.383	0.423	0.459	0.447	0.443

(b) Flores D05: Correlation coefficient between EM_v and EC_e

Depth (cm)	L_0 (current protocols)	L_1	L_2	L_3	L_4	L_5
0–30	0.264	0.291	0.352	0.339	0.345	0.287
0–60	0.208	0.236	0.447	0.406	0.557	0.498
0–90	0.335	0.553	0.532	0.502	0.621	0.564
0–120	0.373	0.572	0.557	0.572	0.633	0.593
0–150	0.411	0.543	0.556	0.757	**0.789**	0.709

L_0 is the soil core location 0 cm perpendicular to the drip line, L_1 is 0.3 m perpendicular to the drip line, L_2 is 0.6 m, L_3 is 0.9 m, L_4 is 1.2 m, and L_5 is 1.5 m perpendicular to the drip line. Bold type indicates the highest correlation coefficient at a given depth. EM_h refers to the measurement of EC_a in the horizontal coil configuration (dS m^{-1}). EM_v refers to the measurement of EC_a in the horizontal coil configuration (dS m^{-1}). EC_e refers to the electrical conductivity of the saturation extract (dS m^{-1}).

Table 8
Correlation coefficients between (a) EM_h and EC_e and (b) EM_v and EC_e for various soil core combinations (i.e., $L_0 + L_1$, $L_0 + L_2$, $L_0 + L_3$, $L_0 + L_4$, and $L_0 + L_5$) at depths of 0–30, 0–60, 0–90, 0–120, and 0–150 cm taken at site Flores D01. 'Current protocols' refers to the protocols presented by Corwin and Lesch (2013) for apparent soil electrical conductivity (EC_a) directed soil sampling of drip irrigated fields, which calibrates EC_a to EC_e using a single soil core taken from directly below the drip line (i.e., L_0).

(a) Flores D05: Correlation coefficient between EM_h and EC_e

Depth (cm)	L_0 (current protocols)	$L_0 + L_1$	$L_0 + L_2$	$L_0 + L_3$	$L_0 + L_4$	$L_0 + L_5$
0–30	0.269	0.361	0.199	0.569	0.500	0.239
0–60	0.271	0.288	0.205	0.655	0.709	0.555
0–90	0.404	0.457	0.521	0.667	0.665	**0.783**
0–120	0.379	0.429	0.411	0.657	0.655	0.528
0–150	0.242	0.302	0.325	0.345	0.301	0.301

(b) Flores D05: Correlation coefficient between EM_v and EC_e

Depth (cm)	L_0 (current protocols)	$L_0 + L_1$	$L_0 + L_2$	$L_0 + L_3$	$L_0 + L_4$	$L_0 + L_5$
0–30	0.264	0.269	0.217	0.276	0.223	0.255
0–60	0.208	0.222	0.449	0.398	0.545	0.567
0–90	0.335	0.521	0.527	0.437	0.576	0.499
0–120	0.373	0.568	0.550	0.512	0.577	0.579
0–150	0.411	0.539	0.512	0.523	0.649	**0.740**

L_0 is the soil core location 0 cm perpendicular to the drip line, L_1 is 0.3 m perpendicular to the drip line, L_2 is 0.6 m, L_3 is 0.9 m, L_4 is 1.2 m, and L_5 is 1.5 m perpendicular to the drip line. Bold type indicates the highest correlation coefficient at a given depth. EM_h refers to the measurement of EC_a in the horizontal coil configuration (dS m^{-1}). EM_v refers to the measurement of EC_a in the horizontal coil configuration (dS m^{-1}). EC_e refers to the electrical conductivity of the saturation extract (dS m^{-1}).

3.2. Modified EC_a-directed soil sampling survey protocols for drip irrigation

The original EC_a-directed soil sampling protocols for fields under drip irrigation by Corwin and Lesch (2013) were developed from a drip-irrigated vineyard in northern California's Napa Valley. Simply stated, the protocols recommended that two separate EC_a surveys should be conducted with one survey consisting of EC_a measurements taken every 3–5 m along the drip lines and the second survey taken between the drip lines (i.e., the crop inter-row). Using a model-based sampling design (i.e., ESAP by Lesch et al., 2000) based on the EC_a measurements, 6–12 (or more depending on the spatial variability of the EC_a measurements) soil cores locations were selected for each of the two surveys. In the case of the EC_a survey taken along the drip lines the soil cores were taken directly below the drip line, which corresponds to L_0 in Tables 1–8. However, in every instance for the salt-affected pistachio orchard at Flores Farm, L_0 provided the lowest correlation with EC_a for D01 and D05 (Tables 1 and 5, respectively). The failure of the Corwin and Lesch (2013) drip-irrigation protocols for the Flores pistachio orchard sites (D01 and D05) is because the Napa Valley vineyard site did not have dramatic salinity gradients near the drip lines like those depicted in Figs. 7 and 8 for the Flores pistachio orchard. The Napa Valley vineyard was situated on a hillside with an impermeable clay layer located approximately 1 m below the soil surface. The topography and impermeable layer resulted in an upslope recharge and a downslope discharge during the rainy months of the winter. Sufficient rainfall was received during the rainy season to leach most of the salts in the root zone downslope to catchment basins. The salinity gradient that existed near the drip line was not as dramatic a gradient as found in well-established drip-irrigated fields of the San Joaquin Valley, such as the Flores pistachio orchard. Subsequently, correlations between EC_a and EC_e at the Napa Valley site were high even though the soil cores associated with the drip-line EC_a survey were taken directly below the drip line in the L_0 position.

It is obvious from the data presented in Tables 1and 5 that soil cores taken in the L_0 position to develop an EC_a-EC_e calibration for the drip-line EC_a survey are problematic in cases where drip irrigation has occurred for more than a decade resulting in substantial lateral salinity gradients. In these instances, the data suggests that a single soil core should be taken at a location perpendicular to the drip line that is 60–80% of the canopy radius. In summary, the following modified EC_a-directed soil sampling protocols for drip irrigation fields are recommended: (1) conduct two separate EC_a surveys with one along the drip line and the other between the drip lines (i.e., the crop inter-row), (2) using a model-based sampling design select 6–12 soil core locations for each of the two EC_a data sets, (3) for the drip-line EC_a data set take the soil core samples at a location perpendicular to the drip line from the base of the plant trunk that is a distance of 0.6–0.8 times the radius of the tree canopy, (4) if sufficient resources are available to take soil cores at two locations instead of one location, then take the soil cores below the drip line and at the edge of the tree canopy (note that two soil cores were not shown to provide an improvement in the EC_a – EC_e calibration), (5) take the soil core samples at 0.3 m increments to a depth of at least 1.2 m, or preferably 1.5 m, (6) if possible, take soil bulk density samples at each depth increment for at least one of the 6–12 soil core sites, (7) analyze soil cores for EC_e, SP and water content, (8) using the DPPC module of ESAP (Lesch et al., 2000) conduct a QA/QC of the data to check the data's reliability and to remove spurious data, and (9) develop an EC_a - EC_e calibration following the guidelines of Corwin and Lesch (2003, 2005b, 2013). From model simulations with HYDRUS-2D, Bughici et al. (2020) recommend an alternative to Step #1, which is to take the geospatial EC_a measurements with the EM38 and associated soil core samples at a distance from the drip line of 1.0 m rather than taking the measurements along the drip line. This alternative would make the EC_a survey easier to take, but it is not recommended at this time until sufficient field data can be collected to establish that it is as reliable and accurate as the proposed Step #1.

An EC_a – EC_e calibration for D01 and D05 was developed using the general calibration equation form shown in Eq. (2):

$$EC_e = EM_hEC_a + EM_vEC_a + x + y + \varepsilon \quad (2)$$

where EC_e is the electrical conductivity of the saturation extract (dS m^{-1}), EM_hEC_a is the apparent soil electrical conductivity measured in the horizontal coil configuration with the EM38 (dS m^{-1}), EM_vEC_a is the apparent soil electrical conductivity measured in the vertical coil configuration with the EM38 (dS m^{-1}), x is the x-coordinate (m), y is the y-coordinate (m), and ε is the error term. The x- and y-coordinates in Eq. (2) account for field-scale trends due to position in the field. The calibration equations using the modified protocols (i.e., core sample taken at the L_4 position) showed a marked improvement over the Corwin and Lesch (2013) protocols (i.e., core sample taken at the L_0 position). Calibration of EC_a to EC_e, improved from $R^2 = 0.25$ to $R^2 = 0.73$ for site Flores D01, and from $R^2 = 0.17$ to $R^2 = 0.72$ for site Flores D05.

4. Summary and conclusions

The local-scale variability in soil salinity found near drip lines in fields that have been under drip irrigation for a decade or longer presents a challenge to mapping salinity with EC_a-directed soil sampling because of the significant salinity gradients that occur both laterally and vertically from the drip line. The challenge of mapping local-scale variability under micro-irrigation with EC_a-directed soil sampling is confirmed by the results presented in Tables 1–8 and points to the need for additional guidelines. Results indicate that the local-scale 3-dimensional complexity of soil salinity patterns near drip lines adds another level of difficulty to the identification of soil core locations for calibrating EC_a to EC_e since the soil core (or cores) must be located at a position that reflects the overall salinity in the volume of measurement of the EM38 instrument (or electrical resistivity device).

The initial EC_a-directed soil sampling protocols for drip irrigation by Corwin and Lesch (2013) were not developed for the dramatic local-scale salinity gradients that occur near drip lines for fields that have been under drip irrigation for long time periods and do not receive sufficient precipitation to leach out salts that accumulate in patterns reflected in Fig. 1. This is confirmed by the data presented. As shown by the L_0 data of Tables 1 and 5, the original protocols failed for this situation. The empirical results of D01 and D05 indicate that the use of Eq. (1) to aid in locating the best position to take a soil core sample or combination of core samples is helpful but may not be sufficient. Eq. (1) shows the core location to be between 0.6 and 1.2 m. The empirical data shows that a single soil core taken at L_3 or L_4, which corresponds to 60–80% of the canopy radius (i.e., 0.9–1.2 m), is best for the crop (mature pistachio orchard) and soil conditions at Flores Farm. If two soil cores are taken and composited, then cores $L_0 + L_5$ are best, but do not necessarily provide better results than a single core. Composites of $L_3 + L_4$ are also reasonably good.

It is dubious that the modified EC_a-directed soil sampling protocols can be applied to other crops and soil conditions. Conducting this type of study for each drip irrigated crop and different soil conditions is impractical. The use of 2-D solute transport models such as HYDRUS-2D provides a means of determining soil salinity distributions under drip irrigation to identify where soil cores are best taken. The paper by Bughici et al. (2020) shows how this is accomplished. The conclusion of Bughici et al. (2020) falls in line with the empirical findings of our paper. Bughici et al. (2020) concluded that for a crop, soil conditions, and irrigation water quality like what occurred at Flores pistachio orchard the distance from the drip line for EM38 EC_a measurements and associated soil samples should be taken 1.0 m perpendicular to the drip line beneath the tree, which matches closely with the 0.6–0.8 times the canopy radius (or 0.9–1.2 m) found herein. However, further research needs to be conducted to determine if geospatial measurements of EC_a taken parallel to the drip line at a distance of 0.6–0.8 times the canopy radius (0.9–1.2 m from the drip line) or as Bughici et al. (2020) recommend at a distance 1.0 m from the drip line are viable alternatives to taking the geospatial measurements along the drip line. In addition, research needs to be conducted to validate the modeling approach for a variety of other drip irrigated crops, soil conditions, and irrigation water qualities.

Maps of soil salinity are among the most valuable tools for irrigation management and salt leaching practices in water-scarce agricultural areas such as California's San Joaquin Valley, Imperial Valley, and Coachella Valley. The increased use of micro-irrigation systems in water-scarce agricultural areas to cope with climate change impacts causing more extreme drought conditions is a significant challenge to map soil salinity for managing these more water-efficient irrigation systems. The potential ramifications of creating soil salinity maps of drip-irrigated fields that delineate accurate and reliable local- and field-scale soil salinity distributions within the root zone are greater crop productivity using less water of lower water quality.

Declaration of Competing Interest

The authors declare that they have no known competing financial interests or personal relationships that could have appeared to influence the work reported in this paper.

Acknowledgments

The authors acknowledge the assistance of several scientists, technicians, and field personnel whose hard work and technical capabilities resulted in the success of the field study at Flores Orchards. These individuals include Catherine Mae Culumber, Blake Sanden, Tait Rounsaville, Paul Markley, Devin Politoske, Towfiqur Khan, Brian Rojas-Lerena, Michael Whiting, Giulia Marino, Matt Reed, and Kristen Shapiro. The authors also acknowledge two grants that helped fund a substantial portion of the field expenses to collect soil core samples: (1) grant award # SCB15040 (California Department of Food and Agriculture – Specialty Crop Block Program, USA, 2015) and (2) grant award # UC 3-77B-79 (California Pistachio Research Board, USA, 2018).

References

Bughici, T., Skaggs, T. H., Corwin, D. L., Zaccaria, D. A., & Scudiero, E. (2020) Ensemble Modeling of Soil Water and Solute Dynamics for Salinity Mapping and Management in Drip-Irrigated Tree Orchards [Abstract]. ASA, CSSA and SSSA International Annual Meetings (2020) | VIRTUAL, Phoenix, AZ. https://scisoc.confex.com/scisoc/2020am/meetingapp.cgi/Paper/125741.

Burt, C.M., Isbell, B., 2005. Leaching of accumulated soil salinity under drip irrigation. Trans. ASAE 48 (6), 2115–2121.

Corwin, D.L. 2005. Geospatial measurements of apparent soil electrical conductivity for characterizing soil spatial variability. In: Álvarez-Benedí, J., Muñoz-Carpena, R. (eds.), Soil-Water-Solute Characterization: An Integrated Approach. CRC Press, Boca Raton, FL, pp. 640–672.

Corwin, D.L., 2021. Impact of climate change on soil salinity in agricultural areas. Eur. J. Soil Sci. 72, 842–862. https://doi.org/10.1111/ejss.13010.

Corwin, D.L., Lesch, S.M., 2003. Application of soil electrical conductivity to precision agriculture: theory, principles, and guidelines. Agron. J. 95, 455–471.

Corwin, D.L., Leach, S.M., 2005a. Apparent soil electrical conductivity measurements in agriculture. Comput. Electron. Agric. 46, 11–43.

Corwin, D.L., Lesch, S.M., 2005b. Characterizing soil spatial variability with apparent soil electrical conductivity: I. Survey protocols. Comput. Electron. Agric. 46 (1–3), 103–133.

Corwin, D.L., Lesch, S.M., 2005c. Characterizing soil spatial variability with apparent soil electrical conductivity: II. Case study. Comput. Electron. Agric. 46 (1–3), 135–152.

Corwin, D.L., Lesch, S.M., 2013. Protocols and guidelines for field-scale measurement of soil salinity distribution with EC_a-directed soil sampling. J. Environ. Eng. Geophys. 18 (1), 1–25.

Corwin, D.L., Scudiero, E., 2020. Field-scale apparent soil electrical conductivity. Soil Sci. Soc. Am. J. 84, 1405–1441. https://doi.org/10.1002/saj2.21153.

Corwin, D.L., Kaffka, S.R., Hopmans, J.W., Mori, Y., Lesch, S.M., Oster, J.D., 2003a. Assessment and field-scale mapping of soil quality properties of a saline-sodic soil. Geoderma 114, 231–259.

Corwin, D.L., Lesch, S.M., Shouse, P.J., Soppe, R., Ayars, J.E., 2003b. Identifying soil properties that influence cotton yield using soil sampling directed by apparent soil electrical conductivity. Agron. J. 95 (2), 352–364.

Dai, A., 2011. Drought under global warming: a review. Wiley Interdiscip. Rev. Clim. Change 2 (1), 45–65. https://doi.org/10.1002/wcc.81.

Food and Agriculture Organization (FAO). 2012. Coping with Water Scarcity. FAO Water Reports No. 38. Food and Agriculture Organization of the United Nations, Rome, Italy.

Food and Agriculture Organization (FAO). 2017. Does Improved Irrigation Technology Save Water? Food and Agriculture Organization of the United Nations, Cairo, Egypt. Available at http://www.fao.org/3/i7090en/I7090EN.pdf (verified Sept. 20, 2021).

Hanson, B., May, D. 2011. Drip irrigation salinity management for row crops. ANR Publication 8447. University of California Agriculture and Natural Resources Communication Services, Richmond, CA. Available at http://anrcatalog.ucdavis.edu.

Jadoon, K.Z., Altaf, M.U., McCabe, M.F., Hoteit, I., Muhammad, N., Moghadas, D., Weihermüller, L., 2017. Inferring soil salinity in a drip irrigation system from multi-configuration EMI measurements using adaptive Markov chain Monte Carlo. Hydrol. Earth Syst. Sci. 21, 5375–5383. https://doi.org/10.5194/hess-21-5375-2017.

Jadoon, K.Z., Moghadas, D., Jadoon, A., Missimer, T.M., Al-Mashharawi, S.K., McCabe, M.F., 2015. Estimation of soil salinity in a drip irrigation system by using joint inversion of multicoil electromagnetic induction measurements. Water Resour. Res. 51, 3490–3504. https://doi.org/10.1002/2014WR016245.

Johnson, C.K., Doran, J.W., Duke, H.R., Weinhold, B.J., Eskridge, K.M., Shanahan, J.F., 2001. Field-scale electrical conductivity mapping for delineating soil condition. Soil Sci. Soc. Am. J. 65, 1829–1837.

Lesch, S.M., Corwin, D.L., Robinson, D.A., 2005. Apparent soil electrical conductivity mapping as an agricultural management tool in arid zone soils. Comput. Electron. Agric. 46 (1–3), 351–378.

Lesch, S.M., Rhoades, J.D., Corwin, D.L. 2000. ESAP-95 Version 2.10R: User and Tutorial Guide. Research Rpt. 146. USDA-ARS, U.S. Salinity Laboratory, Riverside, CA.

Lesch, S.M., Rhoades, J.D., Lund, L.J., Corwin, D.L., 1992. Mapping soil salinity using calibrated electromagnetic measurements. Soil Sci. Soc. Am. J. 56, 540–548.

Qadir, M., Quillerou, E., Nangia, V., Murtaza, G., Singh, M., Thomas, R.J., Drechsel, P., Noble, A.D., 2014. Economics of salt-induced land degradation and restoration. Nat. Resour. Forum 38, 282–295.

Sparks, D.L. (ed.). 1996. Methods of Soil Analysis, Part 3 – Chemical Methods, SSSA Book Series #5, SSSA-ASA, Madison, WI, USA.

Taylor, R., Zilberman, D., 2017. Diffusion of drip irrigation: the case of California. Appl. Econ. Perspect. Policy 39 (1), 16–40.

Tindula, G.N., Orang, M.N., Snyder, R.L., 2013. Survey of irrigation methods in California in 2010. J. Irrig. Drain. Eng. 139 (3) https://doi.org/10.1061/(ASCE)IR.1943-4774.0000538.

Welle, P.D., Mauter, M.S., 2017. High-resolution model for estimating the economic and policy implications of agricultural soil salinization in California. Environ. Res. Lett. 12.

Williams, A.P., Cook, B.I., Smerdon, J.E. 2022. Rapid intensification of th emerging southwestern North American megadrought in 2020–2021. Nat. Clim. Chang. https://doi.org/10.1038/s41558–022-01290-z.